

Finding optimal Pulse Repetition Intervals with Many-objective Evolutionary Algorithms

Paul Dufossé^{*†‡}, Cyrille Enderli^{*}

^{*}Thales DMS, France

[†]Randopt team, Inria Paris-Saclay, France

[‡]Centre de Mathématiques Appliquées de Polytechnique, IP Paris, France

Abstract—In this paper we consider the problem of finding Pulse Repetition Intervals allowing the best compromises mitigating range and Doppler ambiguities in a Pulsed-Doppler radar system. We revisit a problem that was proposed to the Evolutionary Computation community as a real-world case to test Many-objective Optimization algorithms. We use it as a baseline to compare several Evolutionary Algorithms for black-box optimization with different metrics. Resulting data is aggregated to build a reference set of Pareto optimal points and is the starting point for further analysis and operational use by the radar designer.

Keywords—*Medium PRF Radar, Pulsed-Doppler Radar, Evolutionary Algorithms, Multi Objective Optimization, Black-box Optimisation, Benchmarking*

INTRODUCTION

Airborne Pulsed-Doppler radars are complex systems and have been further developed for decades by engineers. While this field is still improving through theoretical findings and ad hoc processing techniques, today's computational means and global optimization techniques need to be considered as another way of opening the black box. The problem of finding Pulse Repetition Intervals (PRIs, or equivalently Pulse Repetition Frequencies - PRF [15]) is not recent and has already been treated with many search heuristics. Here we propose to generate an exhaustive set of solutions to better understand the trade-offs. Almost all Pulsed-Doppler radars operate at medium PRF (between 3 kHz to 30 kHz) hence produce ambiguous range and Doppler measures. The common technique to overcome this situation is to construct a waveform consisting of a train of pulses with multiple PRF. Researchers already found several sets of PRF designing various search heuristics:

In [15] the author finds a set of PRF guided by a constraint programming approach: first generating a set of feasible candidates, then sequentially testing the candidates with 3 scoring passes, finally examining blind zones plots. The AN/APG-69 radar system is chosen as a baseline and the paper ends mentioning a single choice of a PRF set of size 8.

In 2003 [2] C. Alabaster and E. Hughes proved the efficiency of Evolution Algorithms to identify near-optimal PRF sets with 8 or 9 for a practical fire control radar system. E. Hughes would later propose a similar problem under the scope of Many-objective optimization that we will detail in Section I.

In [1] was proposed a model that is similar to the one considered here, with a constant duty cycle but a somehow different parameters setting (smaller dwell time, smaller Doppler interval ...) and aims at minimizing the blind zones while ensuring full decodability in the zone of interest. A single solution set of 8 PRIs is found using a Simulated Annealing approach.

In this paper we propose to revisit a radar PRI design problem proposed 13 years ago and stated as a Multi Objective Optimization problem (MOP). We generate candidate solutions with state-of-the-art evolutionary algorithms and have a glance at how one can assess performance in this context. Our contributions can be summarized as follows:

- Augmented Reference sets for the problem at hand (we found new optimal points)
- Pareto Front Analysis that allows the radar designer to better understand the trade-offs
- Benchmarking Evolutionary Multi Objective Optimization (EMO) algorithms on a real-world problem

The paper is organised as follows: in Section I we remind the considered problem, then we detail the algorithms and metrics used for EMO in Section II. Experimental results and analysis are presented in Section III and Section IV concludes the work and possible extensions.

Notations

We denote by $\mathbf{x} = [x_1, \dots, x_D]^T$ an arbitrary real column-vector (also called a *point* in the D -dimensional search space), \mathcal{P} is a set of points $\{\mathbf{x}_1, \dots, \mathbf{x}_{\#\mathcal{P}}\}$ and $\#\mathcal{P}$ its cardinal. We denote as $f(\mathcal{P}) = \{f(\mathbf{x}); \mathbf{x} \in \mathcal{P}\}$ the Pareto Front induced by the set \mathcal{P} . The notion of set used here may not be confused with the common meaning of a set of PRIs, represented here as a the D -dimensional vector.

I. RADAR PROBLEM

In 2007 Evan J. Hughes introduced a real engineering problem to the EMO community [13]. It is a Waveform Design problem for Pulsed Doppler Radar to mitigate the range and Doppler ambiguities. It also accounts for blind zones and total transmission time (or dwell time) The problem is to find a set of PRIs in the integer range $[500, 1500]$, meaning we consider time quantization of $0.1 \mu\text{s}$. The function accepts any continuous value in this range as input and then does implicit rounding. The performance measure is casted as a multivariate,

multivalued real continuous function $f : \mathbb{R}^D \rightarrow \mathbb{R}^M$. It has $M = 9$ objectives and varying dimension for the decision variables $D \in [4, 12]$. The MOP is designed to:

- Reduce ghosting in range (f_1, f_5)
- Reduce ghosting in velocity (f_2, f_6)
- Avoid blind ranges (f_3, f_7)
- Avoid blind velocities (f_4, f_8)
- Minimize dwell time (f_9 , to be ≤ 50 ms)

Note that each underlying goal translates to 2 objectives as we optimize respectively for the median (f_1 to f_4) and minimum (f_5 to f_8) values. This suggests that the set of objective functions are not totally independent. The software to call this function is available in Matlab as a proprietary executable and therefore the code cannot be read nor modified. An exhaustive list of the radar model's characteristics from [13] is reproduced in Table I for the reader's convenience.

Parameter	Value
Carrier frequency	9.97 GHz for first PRF, each following -30MHz
Minimum PRI	50 μ s
Maximum PRI	150 μ s
Compressed pulsewidth	0.5 μ s
Receiver recovery time	1.0 μ s
Range resolution	75 m
FFT size	64 bins
Duty cycle	10% fixed
Maximum target dwell time	50 ms
Maximum target velocity	± 1500 ms $^{-1}$
Maximum detection range	185.2 km
Number of PRFs	4 to 12 (10 in this paper)
Number of PRFs for coincidence	3

TABLE I: The (proprietary) code internal model's characteristics

II. EVOLUTIONARY MANY OBJECTIVE OPTIMIZATION

A. Preliminaries

EMO is a growing field among Evolutionary Computation and has been successfully applied to solve real-world problems. We consider the problem described above as a Multi Objective Optimization Problem (MOP) of the form:

(jointly) minimize $f(\mathbf{x}) = (f_1(\mathbf{x}), \dots, f_M(\mathbf{x}))$ subject to $\mathbf{x} \in \mathbf{X}$

where $\mathbf{X} \subset \mathbb{R}^D$ is the feasible space for the PRIs. Constraint handling is a nontrivial subject and here we shall restrict ourselves to bound constraints of the form $\mathbf{X} = \{\mathbf{x} \in \mathbb{R}^D, 500 \leq \mathbf{x}_i \leq 1500, i = 1, \dots, D\}$. Here the terminology of Many Objective Optimization Problem (MaOP) is used because $M \geq 4$. The problem is said to be black-box as no other additional information (e.g. gradient, hessian) is available to the optimization algorithm. Evolutionary Algorithms (EAs) are meta-heuristic optimization algorithms specifically designed to handle such problems. They proved efficient to solve non-convex, multi-modal, and non-differentiable problems. In this paper we consider EAs extensions to solve MOPs, namely MOEAs. Recall the objective function is multivalued and the different objectives are conflicting. In this context the MOEAs are appealing as they output a set of Pareto-optimal solutions.

Pareto dominance: Let $\mathbf{x}, \mathbf{y} \in \mathbf{X}$, then we say that \mathbf{x} dominates \mathbf{y} , denoted $\mathbf{x} \succ \mathbf{y}$ if and only if $\forall i f_i(\mathbf{x}) \leq f_i(\mathbf{y})$ and $\exists i f_i(\mathbf{x}) < f_i(\mathbf{y})$. In a set \mathcal{P} , a point \mathbf{x} is said to be non-dominated if no point in \mathcal{P} dominates \mathbf{x} .

Popular MOEAs rely on non-dominated sorting to select preferred candidate solutions. It is well known that, when it comes to MaOPs (increasing number of objectives), the Pareto dominance relationship is not enough to ensure selection pressure, as most sampled points become non-dominated.

The initial population is an input to the algorithm, and can be either randomly sampled or given by a domain-specific heuristic.

B. Performance assessment

It is not straightforward to evaluate algorithm performance for MOPs and MaOPs, and even more difficult when the true Pareto Front is not known. There exist several ways to characterize performance, leading to conflicting results [3]. The PlatEMO manual [17] suggests to use the final population. This is different from what is recommended in [7] for assessing performance on bi-objective problems, where one uses all non-dominated points seen during the process (using the archive). Here we rely on this latter approach to build sets of non-dominated points for each algorithm.

1) *Building the Reference set:* We maintain an archive \mathcal{A} of all points sampled during each algorithm's search process. Concatenating sets of non-dominated points from different algorithms and do a non-dominated sorting to obtain the (reference) best set \mathcal{B} , and $f(\mathcal{B})$ the so-called Empirical Pareto Front (EPF). In other words this is the set containing all non-dominated points seen so far for the problem at hand as in a real-world context we don't know the true PF.

2) *Scaling:* Before each metric is computed, we transform the objective space, each coordinate is scaled from $[m_i, \bar{m}_i]$ to $[0, 1]$, computing \tilde{f} as follows:

$$\tilde{f}_i(\mathbf{x}) = \frac{f_i(\mathbf{x}) - m_i}{\bar{m}_i - m_i} \text{ where } m_i = \min_{\mathbf{x} \in \mathcal{B}} f_i(\mathbf{x}), \bar{m}_i = \max_{\mathbf{x} \in \mathcal{B}} f_i(\mathbf{x})$$

3) *Metrics:* To assess the quality of a set of points \mathcal{P} against \mathcal{B} we propose to use metrics computed in the objective space, comparing $f(\mathcal{P})$ to $f(\mathcal{B})$:

- *Cardinality* The number of non-dominated points is not a reliable quality indicator, as most points are non-dominated, an algorithm could sample many non-dominated points from only a small connected area of the Pareto Set. Still it appears interesting to view, from all the non-dominated points sampled by an algorithm, how many are kept in the final best set \mathcal{B} .
- The *Hypervolume* (HV) [8] of the considered set with respect to a reference point \mathbf{r} . The hypervolume is maximal when considering the continuous True Pareto Front. The construction of the best set leads to $HV_c(\mathcal{B}) \geq HV_c(\mathcal{P})$ for any set \mathcal{P} from a single algorithm. The greater the hypervolume, the better the PF is covered. The reference point can be the nadir point (the vector composed with the worst objectives values over the

Pareto Front, here $[1, \dots, 1]$ after scaling) or another point of interest.

$$\text{HV}_{\mathbf{r}}(\mathcal{P}) = \text{VOL}(\cup_{\mathbf{x} \in \mathcal{P}} [\tilde{f}_1(\mathbf{x}), \mathbf{r}_1] \times \dots \times [\tilde{f}_M(\mathbf{x}), \mathbf{r}_M])$$

where $\text{VOL}(\cdot)$ is the usual Lebesgue measure. In the PlatEMO framework, when the number of objectives M is greater than 4, we do not compute exact hypervolume but rather estimate it by Monte Carlo approximation with 1,000,000 sampled points. We slightly abuse our notation and denote by HV_c the hypervolume with reference point $\mathbf{r} = c \cdot [1, \dots, 1]$.

- *Generational and Inverted Generational Distances* (rsp. IGD, GD) [4] compare two sets of solutions. Here we always compare a set \mathcal{P} to the EPF \mathcal{B} .

$$\text{IGD}(\mathcal{P}, \mathcal{B}) = \frac{1}{\#\mathcal{B}} \sum_{\mathbf{y} \in \mathcal{B}} d_f(\mathbf{y}, \mathcal{P})$$

$$\text{GD}(\mathcal{P}, \mathcal{B}) = \frac{1}{\#\mathcal{P}} \sum_{\mathbf{x} \in \mathcal{P}} d_f(\mathbf{x}, \mathcal{B})$$

where $d_f(\mathbf{y}, \mathcal{P}) = \min_{\mathbf{x} \in \mathcal{P}} \|\mathbf{f}(\mathbf{x}) - \mathbf{f}(\mathbf{y})\|_2$ is the distance in the objective space and $\#\mathcal{P}$ is the set cardinality. IGD iterates over points on the EPF and checks for closest points in \mathcal{P} . IGD is meaningful when there are enough points in the reference set; when the true Pareto Front is known, it makes sense to uniformly sample these points. In our context we only have access to the EPF and such requirements can be seen as limits of the performance assessment using the IGD quality indicator. GD iterates over the set of points to be checked \mathcal{P} . By construction all non-dominated points from \mathcal{P} also belong to \mathcal{B} , then GD penalizes points that turned out to be dominated when compared to the EPF.

C. Algorithms

We rely on a previous study [14] comparing 13 algorithms on classes of problems with 2, 3 or 7 objectives and select 5 promising algorithms to compare with the NSGA-II baseline on the PRIs search problem. Parameters setting follows the experimental setup suggested in [14].

- NSGA-II is one of the oldest and most cited MOEA. It uses Pareto dominance as first sorting procedure and evaluates crowding distance as a second criterion for diversity preservation.
- MSOPS-II [12] is the original algorithm proposed by E. Hughes to solve MaOPs and used for the radar waveform problem [13]. MSOPS is not Pareto-based but a criteria based on predefined target vectors. MSOPS-II adds automatic target vectors generation and clarified fitness assignment
- Indicator Based EA (IBEA) [18] where the search is guided by the (additive) ϵ -indicator. Parameter set is $\kappa = 0.05$.
- NSGA-III [5] is a reference-point based evolutionary algorithm following the NSGA-II framework. Like NSGA-II, it uses first non dominated sorting and then

Algorithm	NSGA-II	NSGA-III	IBEA	GrEA	MSOPS-II	θ -DEA
CPU time	37.6	61.4	53.6	64.5	242.6	55.4

TABLE II: Matlab output for *cputime*, running each algorithm for 100,000 function evaluations, averaged over 10 runs

selects points based on a niche-preservation criterion. These niches are meant to bias the search towards the specified reference points. Here we generate λ reference points uniformly distributed on the unit hyperplane.

- Grid-based EA (GrEA) [9] where the fitness assignment procedure depends on three grid-based criteria. The number of divisions of the objective space in each dimension is set to *div* = 10.
- θ -DEA [10] where the Pareto dominance is replaced by θ dominance, and θ is a penalty parameter, here set to $\theta = 5$. Here again we generate λ reference points uniformly distributed on the unit hyperplane.

III. EXPERIMENTS

A. Algorithms comparison

For all experiments problem dimension has been set to $D = 10$. The initial population is uniformly sampled in $[500, 1500]^D$. We run each algorithm $N_r = 10$ times and each time for a fixed number $N_f = 100,000$ of function evaluations. The population size λ is also fixed to be the same for each algorithm, i.e. $\lambda = 100$. We aggregate points by algorithm, concatenating all archives from the different runs, and keeping all non-dominated points to build each set \mathcal{P} . The computational requirements for each algorithm are quiet the same, as reported in Table II, except for MSOPS-II which is 4 to 5 times longer than average.

From our generated data we obtain a first best set of size 217,166. We also added the set of solutions provided E. Hughes in his original paper [13]. At the end we obtain a final best set $\mathcal{B} = 222,667$ out of 229,016 candidates.

1) *Cardinality metrics*: For each algorithm there is a total of $N_r \times N_f = 1,000,000$ points sampled. We show in Table III the total number of non-dominated points for each algorithm set and its contribution to the overall best set

NSGA-II and NSGA-III are the 2 algorithms that contributed the most to \mathcal{B} in the number of non-dominated points. Yet they also have the lowest ratios of non-dominated points added to \mathcal{B} from their own set. This suggests that the NSGA framework does not converge to a fixed set of points on the PF but is rather moving closed to it, finding new non-dominated points in the high dimensional objective space. This cyclic behaviour is well known from the EMO literature [8]. For comparison, IBEA gives a smaller set \mathcal{P} of non-dominated points, but a large part of it contributes to \mathcal{B} (90.8%). Note that, not only we improved the original dataset by increasing its size, but half of the points provided by the original experiment [13] are now dominated by \mathcal{B} .

Algorithm set	NSGA-II	NSGA-III	IBEA	GrEA	MSOPS-II	θ -DEA	Hughes [13]	\mathcal{B}
$\#\mathcal{P}$	69,512	85,887	21,344	59,699	27,700	44,798	11,850	222,667
$\#(\mathcal{P} \cap \mathcal{B})$	42,406	54,732	19,384	41,165	22,941	36,342	5,712	
$(/\#\mathcal{P})$	(61.0%)	(63.7%)	(90.8%)	(69.0%)	(82.8%)	(81.1%)	(48.2%)	100%

TABLE III: Number of non-dominated points obtained during the optimization proces, total of 1,000,000 function evaluations. The last line shows the amount of solutions which stay non-dominated when compared to others in the best set.

2) *Real-valued metrics*: We follow the methodology described in Section II-B and compare different metrics for each algorithm set. Results are gathered in Table IV. Hypervolume is computed for 3 different reference points $c \in \{0.9, 1, 1.1\}$ and approximation variance has been checked to be acceptable for comparison. We always give the hypervolume of the set \mathcal{B} as a reference, and percentages comparing the hypervolume of any set \mathcal{P} against \mathcal{B} . The idea to look at many reference points is the following: it is known that the hypervolume quality indicator, when consider high dimensional spaces, tends to promote set of points that are mainly located on the boundary of the Pareto Front (as they have a greater contribution to the integral). By comparing the obtained measures (normalized by $HV_c(\mathcal{B})$), we may have a guess about which algorithm is able to generate solution sets being well spread on the PF. As an example, the hypervolume decrease from 62.52% to 41.31% for NSGA-II when switching the ref. point parameter c from 1 to 0.9. Same remark for MSOPS-II (53.76% to 27.44%). The hypervolume of IBEA is much more stable in all situations, and is alsobest performing for any hypervolume measure, whereas NSGA-III is for IGD and NSGA-II for GD. Therefore no algorithm overperforms all others for all metrics considered here.

B. Problem insights

We propose to visualize the set \mathcal{B} to provide a better understanding of the trade-offs involved in radar waveform design. Recall that, for objectives 1 to 8, values are negative because we require minimization of the MaOP; and objective 9 (dwell time) was added an offset of 50 ms.

- The distribution of each objective's values in Figure 3. A remark is the multimodality of distribution for several objectives. But it is not clear if these modes come from exploitation of specific regions of the search space due to algorithms bias or particular shape of the Pareto Front. Also note that some objective values are greater than zero. This has already been mentioned in the original problem description [13] and should be considered as 0 or violation of implicit constraints. Further experiments should account for such constraints.
- Some scatter plots representing 4 (out of 36) 2-D cuts in the Pareto Front in Figure 1. Some objectives appear to be non-conflicting, for instance median velocity blindness (f_4) vs dwell time (f_9). It is quiet simple to figure it out: the radar is frequency-hopping and the ambiguous velocity is $V_a(n) = \frac{\lambda_n}{2x_n}$ where $\lambda_n = c \cdot (1.10^{10} - n \cdot 3.10^7)^{-1}$, $n = 0 \dots 9$ and c the speed of light. Small dwell time implies small PRIs around 50

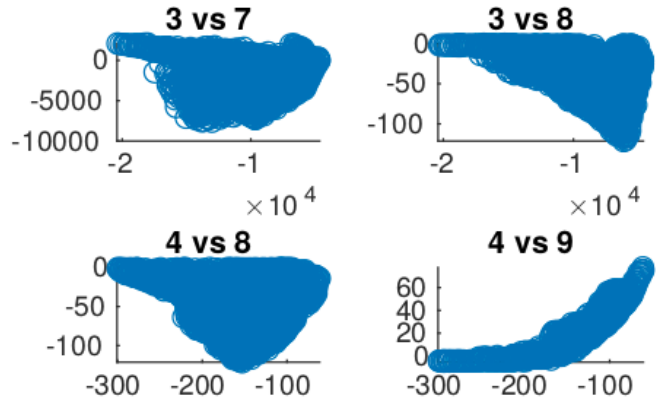


Fig. 1: Points from \mathcal{B} visualized in 2D subspaces, no scaling

μ s. This results in high ambiguous velocities (250 to 300 ms^{-1}). On the contrary, high PRIs (closer to 150 μ s) means smaller ambiguous velocities (around 100 to 120 ms^{-1}). Since targets are searched in the velocity range $\pm 1500 \text{ms}^{-1}$ this explains the observed difference by a factor 2 to 3 (omitting other second-order effects). On the contrary the visualization is less informative for other comparisons, e.g. for f_3 vs f_8 , that is median range blindness vs minimum velocity blindness, one may be able to see the limit cases but there is a large zone that requires higher dimensional views to be clearly explained.

More sophisticated methods exist to better restore information from a high dimensional Pareto Front with different guarantees about what is preserved from the original space [11].

C. Comparison with existing methods

We compared two PRI vectors from the literature with our findings with respect to the baseline problem considered here. These PRIs were find with other methods and meant to solve similar constraints for different radar system parameters settings. They still operate at medium PRF and share common goals. Simpson [15] gives a set of 8 PRF, or equivalently (with proper normalization):

$$\begin{aligned} \mathbf{x}_s &= [19.61, 17.54, 15.87, 15.15, 14.49, 12.82, 11.11, 10.42]^T \text{ kHz} \\ &= [510, 570, 630, 660, 690, 780, 900, 960]^T \times 0.1 \mu\text{s} \end{aligned}$$

Algorithm	NSGA-II	NSGA-III	IBEA	GrEA	MSOPS-II	θ -DEA	Hughes [13]	\mathcal{B}
HV _{0.9} (/HV _{0.9} (\mathcal{B}))	6.94e-4 (41.31%)	7.83e-4 (46.61%)	1.446e-3 (86.07%)	1.048e-3 (62.38%)	4.61e-4 (27.44%)	8.49e-4 (50.54%)	2.16e-4 (18.46%)	1.17e-3
HV ₁ (/HV ₁ (\mathcal{B}))	4.674e-3 (62.52%)	3.458e-3 (46.25%)	7.011e-3 (93.78%)	5.516e-3 (73.78%)	4.019e-3 (53.76%)	3.788e-3 (50.67%)	2.20e-3 (29.33%)	7.5e-3
HV _{1.1} (/HV _{1.1} (\mathcal{B}))	1.3384e-2 (69.81%)	8.795e-3 (45.87%)	1.7343e-2 (90.46%)	1.4815e-2 (77.27%)	1.1972e-2 (62.44%)	9.643e-3 (50.29%)	7.40e-3 (38.54%)	1.92e-2
IGD	6.7534e-2	1.2664e-1	9.1345e-2	7.7832e-2	9.7094e-2	1.4208e-1	1.389e-1	0
GD	1.1245e-4	8.7501e-05	8.8724e-05	1.0369e-4	1.1945e-4	9.2468e-05	3.3103e-04	0

TABLE IV: Computing metrics Hypervolume (HV, to be maximized), Inverted Generational Distance (IGD, to be minimized), Generational Distance (GD, to be minimized). For HV we also display the ratio in percents of HV(\mathcal{P})/HV(\mathcal{B})

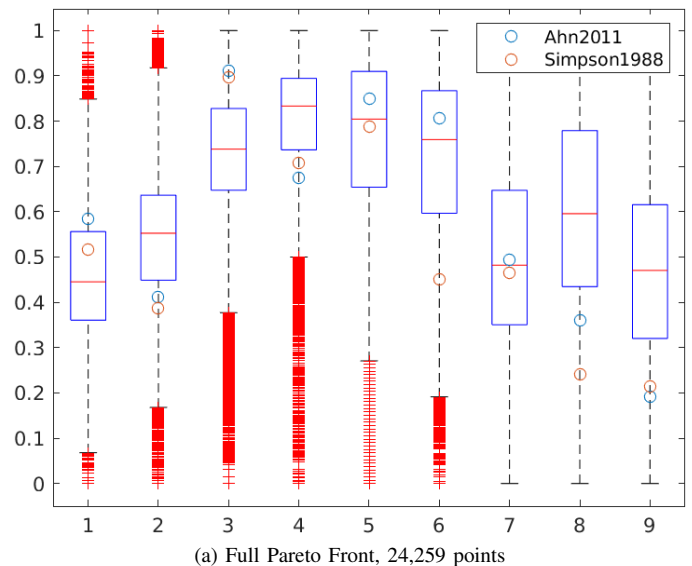
Ahn et al. give a vector of 8 PRIs with a time quantization of 1 μ s:

$$\mathbf{x}_a = [51, 53, 59, 62, 69, 72, 91, 94] \mu\text{s}$$

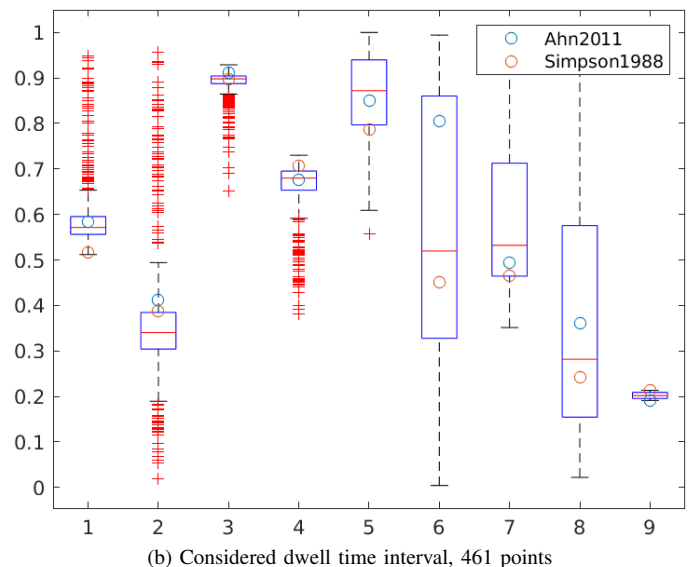
In this comparison we use only IBEA as the most promising algorithm and repeat the previously defined experimental setup to generate $N_r \times N_f = 1,000,000$ points corresponding to 8-tuples of PRIs ($D = 8$). We obtain a set of 24,259 non-dominated points that we use for scaling and the resulting distribution of objective values is shown as boxplots in Figure 2 (a). We also display \mathbf{x}_s and \mathbf{x}_a . Note that the PRIs proposed by Simpson was found to be non-dominated with respect to $\mathcal{P}(\text{IBEA})$, whereas the set proposed by Ahn et al. was dominated. This may be due to the lack of precision resulting from greater time quantization. Note that Simpson's set \mathbf{x}_s is also better performing than \mathbf{x}_a for most of the objectives considered here, except f_4 (median velocity blindness), with a slightly greater dwell time (46.5 ms for \mathbf{x}_s vs 45.4 ms for \mathbf{x}_a). IBEA found 461 points in this dwell time interval (i.e. satisfying $-4.6 < f_9(\mathbf{x}) < -3.5$) and the distribution of objectives for those solutions can be found in Figure 2 (b).

IV. CONCLUSION AND FUTURE WORK

We considered several algorithms *a priori* suited to solve MaOP and benchmarked them on the Radar Waveform problem. We obtained a large collection of non-dominated points that describe the unavoidable trade-offs when designing such radar systems. We also remind this is an *offline* search procedure. These solvers are not aimed at running on the radar hardware, but the obtained PRIs dataset could be used with some specific rules to switch the radar mode while operating. We also illustrated the difficulty of performance assessment when many objectives are involved. Real-world concerns suggest to integrate user preferences through weighted hypervolume: this new measure could lead to different ranking among algorithms. This work could be extended by searching for other numbers of PRIs or refining the objectives. Evolutionary algorithms are black-box by design and prove to be a useful technique for problems related to Radar Signal Processing (see [6], [16]). These results, along with what is known from the Evolutionary Optimisation community, also suggest that CMA-ES as the search operator may be useful to explore Multi-or-Many Objective Optimization of Radar problems.



(a) Full Pareto Front, 24,259 points



(b) Considered dwell time interval, 461 points

Fig. 2: Boxplots of objective values in $\mathcal{P}(\text{IBEA})$, $D = 8$, objective functions are scaled to $[0, 1]$ and to be minimized. Existing PRF sets were added for comparison [1], [15].

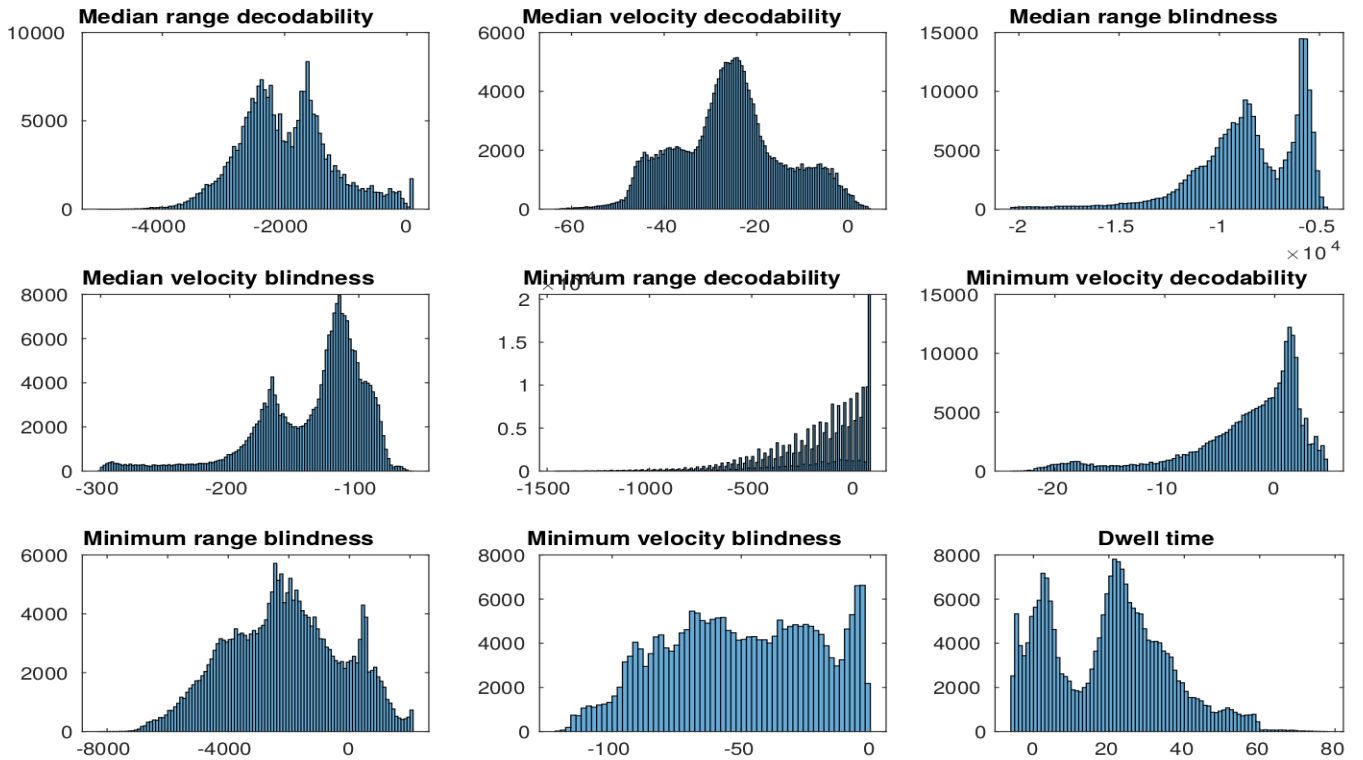


Fig. 3: Histogram of objective values in \mathcal{B} , $D = 10$, objective functions are transformed to appear as a minimization problem: $[-f_1, -f_2, -f_3, -f_4, -f_5, -f_6, -f_7, -f_8, f_9 - 50]$

REFERENCES

- [1] Soyeon Ahn, Heedeok Lee, and Byungwook Jung. Medium prf set selection for pulsed doppler radars using simulated annealing. *IEEE National Radar Conference - Proceedings*, 05 2011.
- [2] Clive Alabaster, Evan Hughes, and J.H. Matthew. Medium prf radar prf selection using evolutionary algorithms. *Aerospace and Electronic Systems, IEEE Transactions on*, 39:990 – 1001, 08 2003.
- [3] C. Audet et al. Performance indicators in multiobjective optimization. working paper or preprint, February 2020.
- [4] C. Coello et al. Solving Multiobjective Optimization Problems Using an Artificial Immune System, 2005.
- [5] K. Deb et al. An Evolutionary Many-Objective Optimization Algorithm Using Reference-Point-Based Nondominated Sorting Approach Part I: Solving Problems With Box Constraints. *IEEE Transactions on Evolutionary Computation*, 18(4):577–601, 2014.
- [6] P. Dufossé et al. Phased-Array Antenna Pattern Optimization with Evolution Strategies. In *2020 IEEE Radar Conference (RadarConf)*, 2020, to be published.
- [7] D. Brockhoff et al. Biobjective performance assessment with the COCO platform. *CoRR*, abs/1605.01746, 2016.
- [8] R. Berghammer et al. Convergence of set-based multi-objective optimization, indicators and deteriorative cycles. *Theoretical Computer Science*, 456:2 – 17, 2012.
- [9] S. Yang et al. A grid-based evolutionary algorithm for many-objective optimization. *IEEE Transactions on Evolutionary Computation*, 17(5):721–736, 2013.
- [10] Y. Yuan et al. A new dominance relation-based evolutionary algorithm for many-objective optimization. *IEEE Transactions on Evolutionary Computation*, 20(1):16–37, 2016.
- [11] B. Filipič et al. Visualization in Multiobjective Optimization. In *Proceedings of the Genetic and Evolutionary Computation Conference Companion, GECCO '19*, page 951–974, New York, NY, USA, 2019. Association for Computing Machinery.
- [12] E. Hughes. MSOPS-II: A general-purpose Many-Objective optimiser. In *2007 IEEE Congress on Evolutionary Computation*, pages 3944 – 3951, 10 2007.
- [13] E. Hughes. Radar Waveform Optimisation as a Many-Objective Application Benchmark. In Shigeru Obayashi, Kalyanmoy Deb, Carlo Poloni, Tomoyuki Hiroyasu, and Tadahiko Murata, editors, *Evolutionary Multi-Criterion Optimization*, pages 700–714, Berlin, Heidelberg, 2007. Springer Berlin Heidelberg.
- [14] K. Li et al. Evolutionary Many-Objective Optimization: A Comparative Study of the State-of-the-Art. *IEEE Access*, 6:26194–26214, 2018.
- [15] J. Simpson. Prf set selection for pulse-doppler radars. In *IEEE Region 5 Conference, 1988: 'Spanning the Peaks of Electrotechnology'*, pages 38–44, 1988.
- [16] U. Tan et al. Optimisation d'un code de phase robuste aux phénomènes d'éclipse. In *GRETSI 2019*, Lille, France, August 2019.
- [17] Ye Tian, Ran Cheng, Xingyi Zhang, and Yaochu Jin. PlatEMO: A MATLAB platform for evolutionary multi-objective optimization. *IEEE Computational Intelligence Magazine*, 12(4):73–87, 2017.
- [18] E. Zitzler et al. Indicator-Based Selection in Multiobjective Search. In *Conference on Parallel Problem Solving from Nature (PPSN VIII)*, pages 832–842, 09 2004.